Asian Journal of Green Chemistry 3 (2019) 258-270

Asian Journal of Green Chemistry

Journal homepage: www.ajgreenchem.com

Original ResearchArticle

Insight into the structural and spectral (IR and UV-Vis) properties of the salts of alkali (Li, Na and K) and alkaline earth (Be, Mg and Ca) metals with pertechnetate oxoanion ($^{99m}TcO_4^-$) as the convenient water-soluble sources of the radioactive element technetium

Mehdi Nabati

Synthesis and Molecular Simulation Laboratory, Chemistry Department, Pars Isotope Company, P.O. Box: 1437663181, Tehran, Iran

ARTICLE INFORMATION

Received: 15August2018
Received in revised: 24 August 2018
Accepted: 24 August 2018
Available online: 31 October 2018

DOI: 10.22034/ajgc.2018.144525.1096

KEYWORDS

Density functional theory
Molecular simulation
Nuclear medicine
Pertechnetate oxoanion
Radiochemistry

ABSTRACT

A quantum mechanical (QM) study is done to unveil the structural and electronic properties and spectroscopy analyses (IR and UV-Vis) of the alkali (Li, Na and K) and alkaline earth (Be, Mg and Ca) salts of the pertechnetate oxoanion ($^{99m}TcO_4^-$) using density functional theory (DFT) method by the popular B3LYP (Becke, three-parameter, Lee-Yang-Parr) exchange correlation functional with 6-31+G(d,p) basis set. Also, the Lanl2DZ effective core potential basis set of theory is used to compute the technetium-99m radioisotopes. The frontier molecular orbitals (FMOs) calculations indicate that the sodium and beryllium salts of pertechnetate anion are more susceptible to react with electron-donating compounds and also, the oxygen atoms, technetium-99m radioisotopes and the cations (Li^+, Na^+, K^+, Be^{2+}, Mg^{2+} and Ca^{2+}) have negative, zero and positive electrostatic potentials, respectively.

Corresponding author,email:mnabati@ymail.com(M. Nabati).
Tel: +982188337023,Fax: +982188337024.

Graphical Abstract

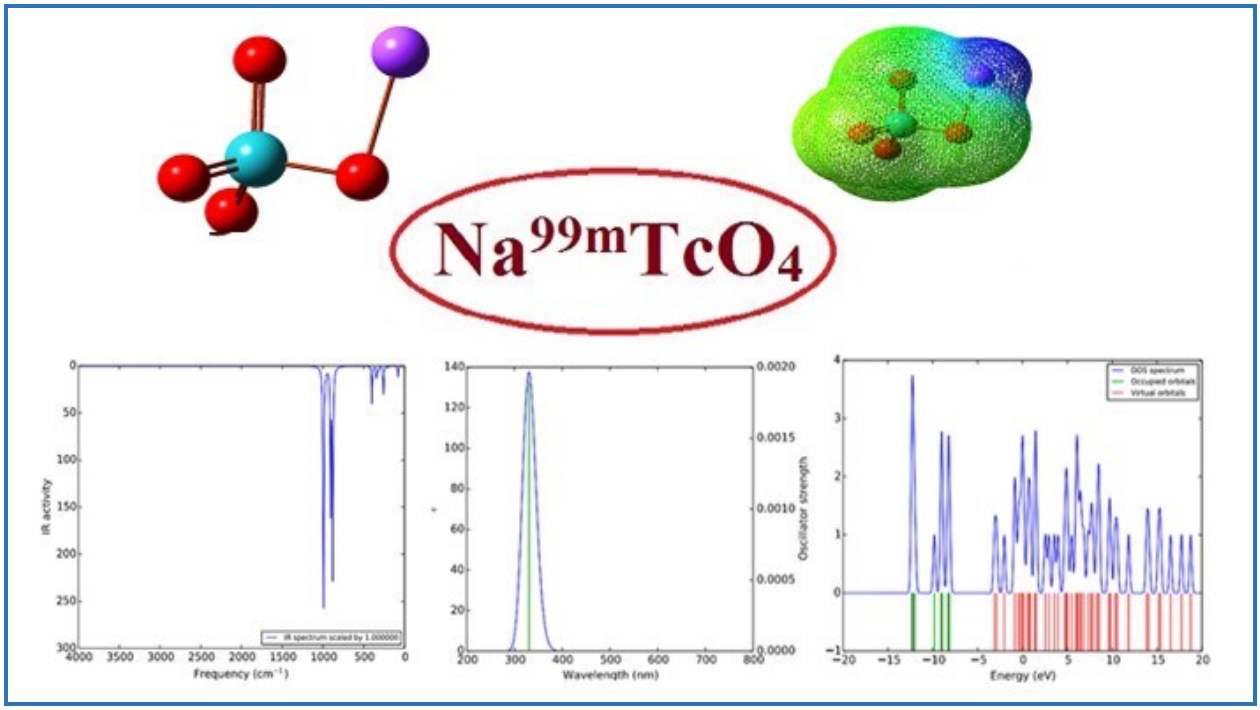

Introduction

A radiopharmaceutical or nuclear medicine is a special type of drug that uses radionuclides to diagnostic and therapeutic goals. The excretion and uptake of these radioisotopes can be detected using the radiopharmaceutical imaging technologies. The two most popular techniques in this area are positron emission tomography (PET) and single photon emission computed tomography (SPECT). The main difference between these two techniques is the type of the used radionuclide. The SPECT scans are used to detect gamma rays and x-rays emitted by radioactive tracers like technetium-99m radioisotope. On the other hand, the PET technology is used to detect the radionuclides with higher energy gamma rays like fluorine-18 radioactive tracer [1–3].

Technetium-99m (Symbolized as ^{99m}Tc) is one of the main radioactive tracers in nuclear medicines area. This radionuclide can be detected in the body internal organs using the SPECT imaging technique. The technetium-99m radionuclide is the decay product of molybdenum-99 radioisotope. This metastable isotope of technetium element (^{99m}Tc) is extracted from a decaying Mo-99 source using a technetium-99m generator (Moly cow or technetium cow) [4]. The molybdenum-99 radioisotope is used in the molybdate (MoO_4^{2-}) form in the moly generator. When the molybdate ion decays, it produces the technetium-99m radioisotope in the form of pertechnetate (TcO_4^-) [5]. The pertechnetate ion is an oxoanion compound that carries the

technetium-99m isotope and is used in a radiopharmaceutical. This oxoanion is the most important starting compound for the technetium chemistry [6]. The pertechnetate ion has various salts that are usually colorless. Sodium pertechnetate is the most famous salt of this oxoanion [7]. The half-life of technetium-99m radionuclide is only six hours. So, the various chemical dimensions of the pertechnetate salts are not known [4–8]. For this reason, the structural and spectral (IR and UV-Vis) properties of the salts of alkali (Li, Na and K) and alkaline earth (Be, Mg and Ca) metals with pertechnetate oxoanion ($^{99m}TcO_4^-$) will be theoretically discussed using density functional theory (DFT) computational method during the presented study.

Experimental

Computational methods

During the presented study, all computations were done using the Gaussian 03 software [9]. The geometries of all of the studied molecules were fully optimized with density functional theory (DFT) computational method by the hybrid B3LYP functional using the 6-31+G(d,p) basis set [10] for the Li, Na, K, Be, Mg, Ca, O, and H atoms and the Lanl2DZ effective core potential basis set for the Tc atoms. The vibrational frequency analyses were carried out to prove that the optimized geometries of the studied compounds were true minima. No imaginary frequency was observed for all of the studied compounds. This confirms the accuracy and correctness of our computations. The graph of the optimized geometries of all molecules, spectral (IR and UV-Vis) analyses, density of states (DOS) and molecular electrostatic potential (MEP) images were obtained using GaussView 6.0.16 and GaussSum 3.0 program packages.

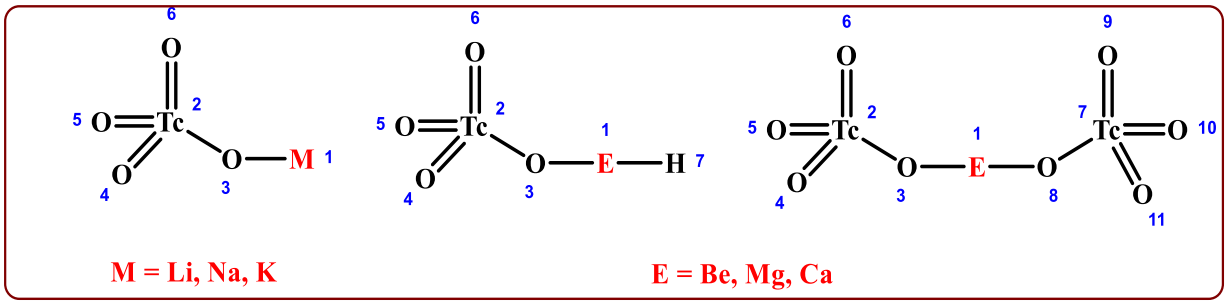

Scheme 1. The molecular structures under study

Results and discussion

Structural study of the pertechnetate salts

Scheme 1 indicates the molecular structure of the salts of alkali (Li, Na and K) and alkaline earth (Be, Mg and Ca) metals with pertechnetate oxoanion ($^{99m}TcO_4^-$). All molecular structures under study were optimized using DFT/B3LYP method with 6-31+G(d,p) basis set and the Lanl2DZ basis set for the technetium atoms.

The optimized molecular structures are shown in Figure 1. The bond lengths data of all of the studied compounds are listed in Table 1. As can be seen from the data, in alkali salts of pertechnetate anion, the M–O and Tc–O3 bond lengths increase and decrease with cation van der waals (VDW) radius increasing, respectively. So, the strength order of M–O (M = Li, Na and K) bonds is Li–O>Na-O>K–O.

We can see from the Table 2, the Li–O, Na-O and K–O bond orders are 0.036, 0.015 and 0.011, respectively. The same increase and decrease in E–O3 and Tc–O3 bond lengths of the monoanion and dianion salts of alkaline earth metals are also observed. On the other hand, the E–H bond length order of monoanion salts is: Ca–H>Mg–H>Be–H. The bond orders 0.668, 0.615 and 0.508 are shown for Be–H, Mg–H and Ca–H bonds, respectively.

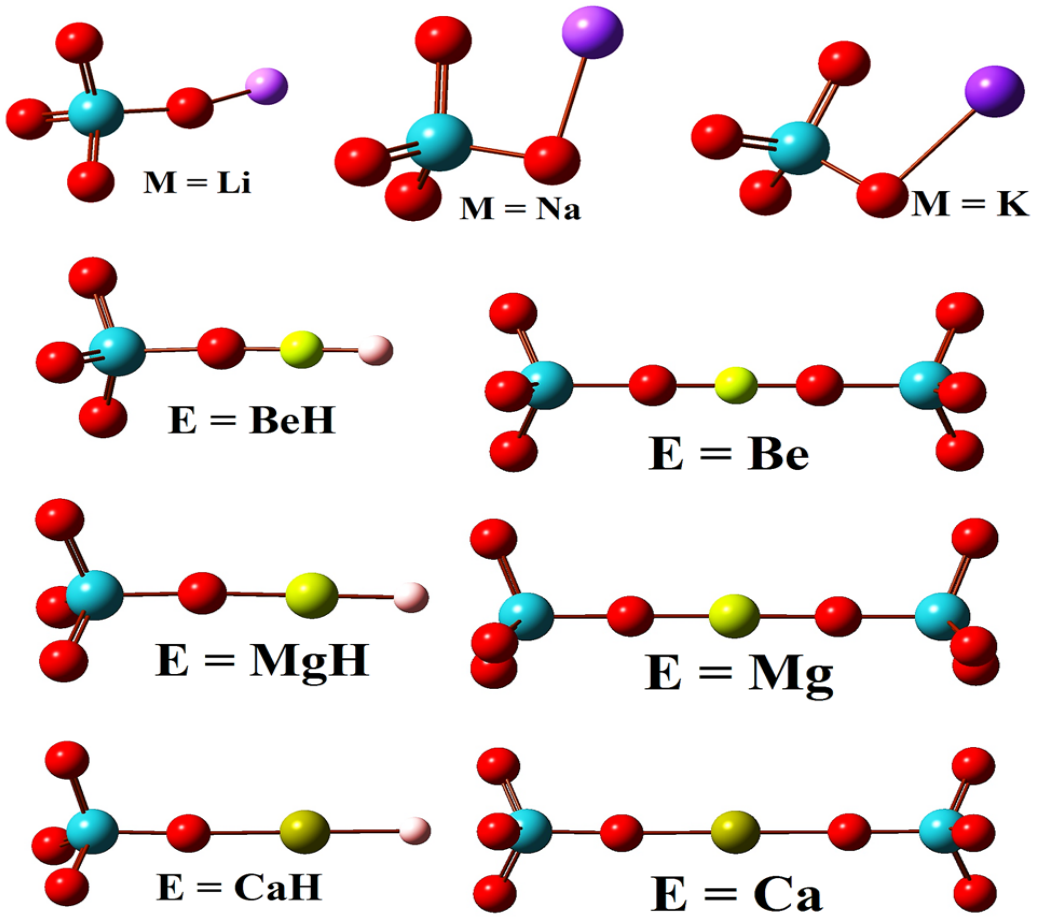

Figure 1. The theoretical geometric structures of the molecules under study

Table 1. Bond lengths data of the molecular structures

Compound	M1-O3	Tc2-O3	Tc2-O4	E1-O3	E1-O8	E1-H7	Tc7-O8	Tc7-O9
M = Li	1.690	1.797	1.711	-	-	-	-	-
M = Na	2.262	1.757	1.758	-	-	-	-	-
M = K	2.613	1.753	1.753	-	-	-	-	-
E = BeH	-	1.851	1.697	1.439	-	1.320	-	-
E = Be	-	1.859	1.696	1.440	1.439	-	1.859	1.696
E = MgH	-	1.823	1.704	1.857	-	1.681	-	-
E = Mg	-	1.834	1.701	1.829	1.829	-	1.834	1.701
E = CaH	-	1.808	1.709	2.199	-	2.077	-	-
E = Ca	-	1.815	1.707	2.173	2.173	-	1.815	1.707

Table 2. Bond orders (B.O.) data of the molecular structures

Compound	M1-O3	Tc2-O3	Tc2-O4	E1-O3	E1-O8	E1-H7	Tc7-O8	Tc7-O9
M = Li	0.036	0.989	1.463	-	-	-	-	-
M = Na	0.015	1.247	1.249	-	-	-	-	-
M = K	0.011	1.263	1.261	-	-	-	-	-
E = BeH	-	0.722	1.546	0.222	-	0.668	-	-
E = Be	-	0.708	1.551	0.213	0.213	-	0.707	1.551
E = MgH	-	0.860	1.504	0.111	-	0.615	-	-
E = Mg	-	0.812	1.518	0.100	0.100	-	0.812	1.519
E = CaH	-	0.942	1.480	0.054	-	0.508	-	-
E = Ca	-	0.911	1.491	0.039	0.039	-	0.911	1.490

Stability and reactivity study

In theoretical chemistry, the highest occupied molecular orbital (HOMO) and the lowest unoccupied molecular orbital (LUMO) are two main types of molecular orbitals that they are called frontier orbitals [11]. The energy difference between these molecular orbitals (HOMO-LUMO gap) can be used to study the stability and reactivity of organic-inorganic compounds [12]. The global reactivity descriptors like chemical hardness (η), chemical softness (S), electronegativity (χ), electronic chemical potential (μ) and electrophilicity index (ω) can be obtained from the energies of the frontier orbitals [11–13]. These reactivity indices are achieved by the following formulas [14]:

$$\eta = \frac{(\varepsilon_{LUMO} - \varepsilon_{HOMO})}{2}$$

$$\chi = \frac{-(\varepsilon_{LUMO} + \varepsilon_{HOMO})}{2}$$

$$\mu = \frac{(\varepsilon_{LUMO} + \varepsilon_{HOMO})}{2}$$

$$\omega = \frac{\mu^2}{2\eta}$$

The frontier orbitals energies and global reactivity indices of the compounds under study have been listed in Table 3. From the data of the Table 3, the stability and chemical hardness orders of the alkali and alkaline earth salts of pertechnetate oxoanione are Li>K>Na and Ca (CaH)>Mg (MgH)>Be (BeH), respectively. It can be deduced that sodium pertechnetate has low stability and chemical hardness property among alkali salts. So, it can be easily reduced by reductant agents such as $SnCl_2$ compound. On the other hand, the electrophilicity index orders of the molecules under study are Na>Li>K and Be (BeH)>Mg (MgH)>Ca (CaH). These orders indicate that the sodium and beryllium salts of pertechnetate anion are more susceptible to react with electron-donating compounds.

Figure 2 indicates the graphs of the density of states (DOS) of the molecules under study. The DOS graphs show that all title compounds are more susceptible to accept electron from other electron-donating compounds. This is due to more density of virtual orbitals to the occupied orbitals. Another important parameter for reactivity determination of organic-inorganic compounds is molecular electrostatic potential (MEP) graph [15].

The MEP graphs of the molecules are gathered in Figure 3. In these graphs, the negative, zero and positive electronic potential areas have been indicated with orange, green and blue colors, respectively. It can be deduced from the MEP graphs, the oxygen atoms, technetium-99m radioisotopes and the cations have negative, zero and positive electrostatic potentials, respectively.

Spectral study of the title compounds

Two important spectroscopic methods for characterization and identification of inorganic molecules are infrared (IR) and UV-Visible spectroscopy (UV-Vis) [16]. Figures 4 and 5 are related to the IR and UV-Vis spectra, respectively.

As can be seen from the Figure 4, the IR spectra of the molecular structures under study show the sharp peaks. Here, the main harmonic frequencies (cm^{-1}) of the structures are discussed.

Table 3. Global reactivity indices of the molecular structures

Compounds	HOMO (eV)	LUMO (eV)	GAP (eV)	χ (eV)	μ (eV)	η (eV)	S $(eV)^{-1}$	ω (eV)
M = Li	-7.93	-2.73	5.20	5.33	-5.33	2.60	0.19	5.46
M = Na	-8.16	-3.12	5.04	5.64	-5.64	2.52	0.20	6.31
M = K	-7.73	-2.56	5.17	5.15	-5.15	2.59	0.19	5.13
E = BeH	-9.53	-4.37	5.16	6.95	-6.95	2.58	0.19	9.36
E = Be	-9.72	-4.64	5.08	7.18	-7.18	2.54	0.20	10.15
E = MgH	-8.76	-3.57	5.19	6.17	-6.17	2.60	0.19	7.34
E = Mg	-9.24	-4.10	5.14	6.67	-6.67	2.57	0.19	8.66
E = CaH	-7.09	-3.19	3.90	5.14	-5.14	1.95	0.26	6.77
E = Ca	-8.79	-3.60	5.19	6.20	-6.20	2.60	0.19	7.41

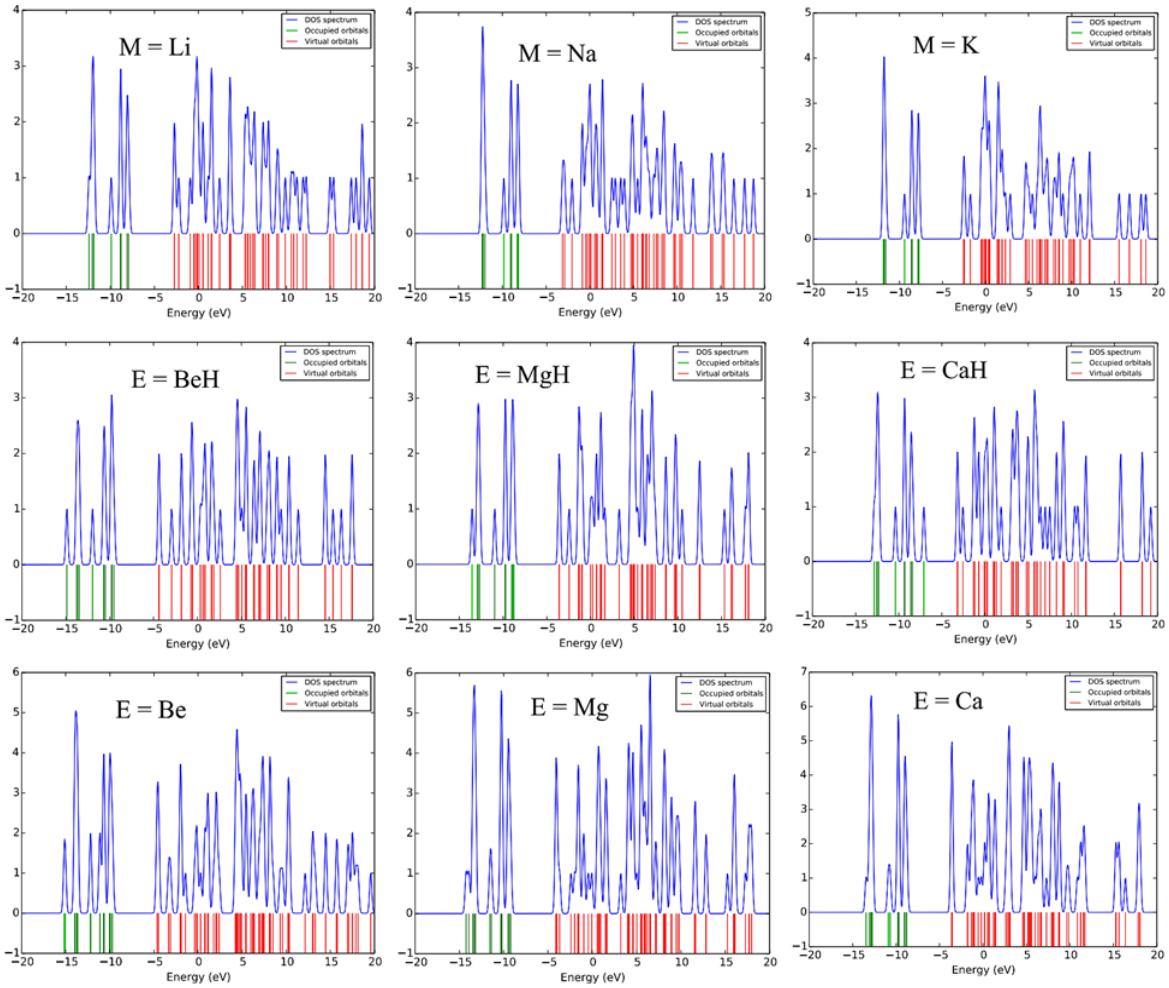

Figure 2. The density of states (DOS) graphs of the molecules under study

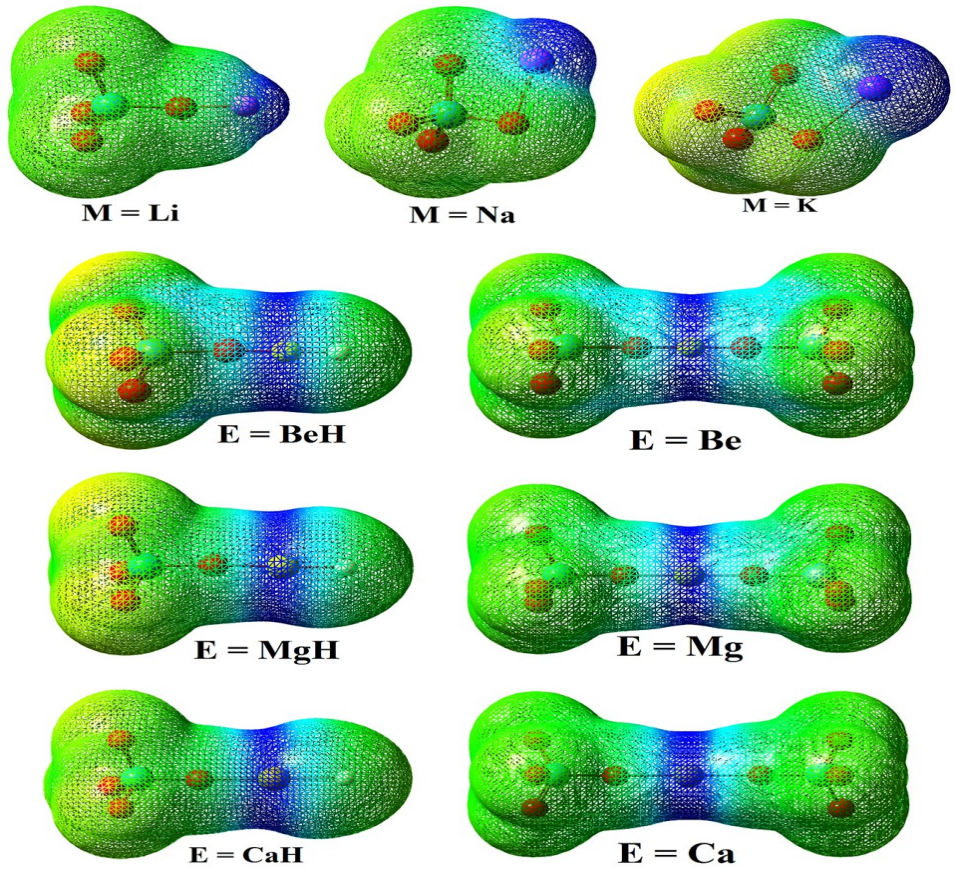

Figure 3. The molecular electrostatic potential (MEP) graphs of the molecules under study

M=Li: 39.1367, 296.8281, 298.6263, 325.7347, 338.1941, 340.6935, 600.9861, 963.4779, 988.9628, 990.1558, and 992.7843.

M=Na: 78.4710, 199.8120, 259.2694, 323.2526, 338.4619, 342.7936, 400.3492, 879.4927, 906.6228, 988.9984, and 996.3728.

M=K: 58.9757, 156.9324, 190.7586, 323.1539, 331.6191, 342.2002, 379.7935, 894.0051, 915.0587, 982.9436, and 990.0596.

E=BeH: 58.4347, 61.8781, 261.0801, 261.5382, 317.7671, 347.1301, 347.5196, 563.4909, 564.8220, 601.6540, 1010.8256, 1010.9332, 1011.1695, 1203.9433, and 2225.7329.

E=Be: 16.7067, 20.6904, 21.9314, 25.8320, 156.0676, 237.0291, 237.1998, 257.7410, 257.9013, 319.8231, 346.3514, 346.7326, 347.1070, 347.4233, 357.3725, 375.3481, 378.3365, 668.6213, 1003.8497, 1006.4453, 1006.5526, 1007.7230, 1007.8586, 1009.1091, 1023.3127, and 1470.0160.

E=MgH: 41.2733, 42.8564, 275.7278, 276.0033, 300.8635, 330.7938, 330.8980, 343.6128, 344.5428, 419.7342, 939.8354, 1000.4057, 1001.8598, 1002.3307, and 1683.2218.

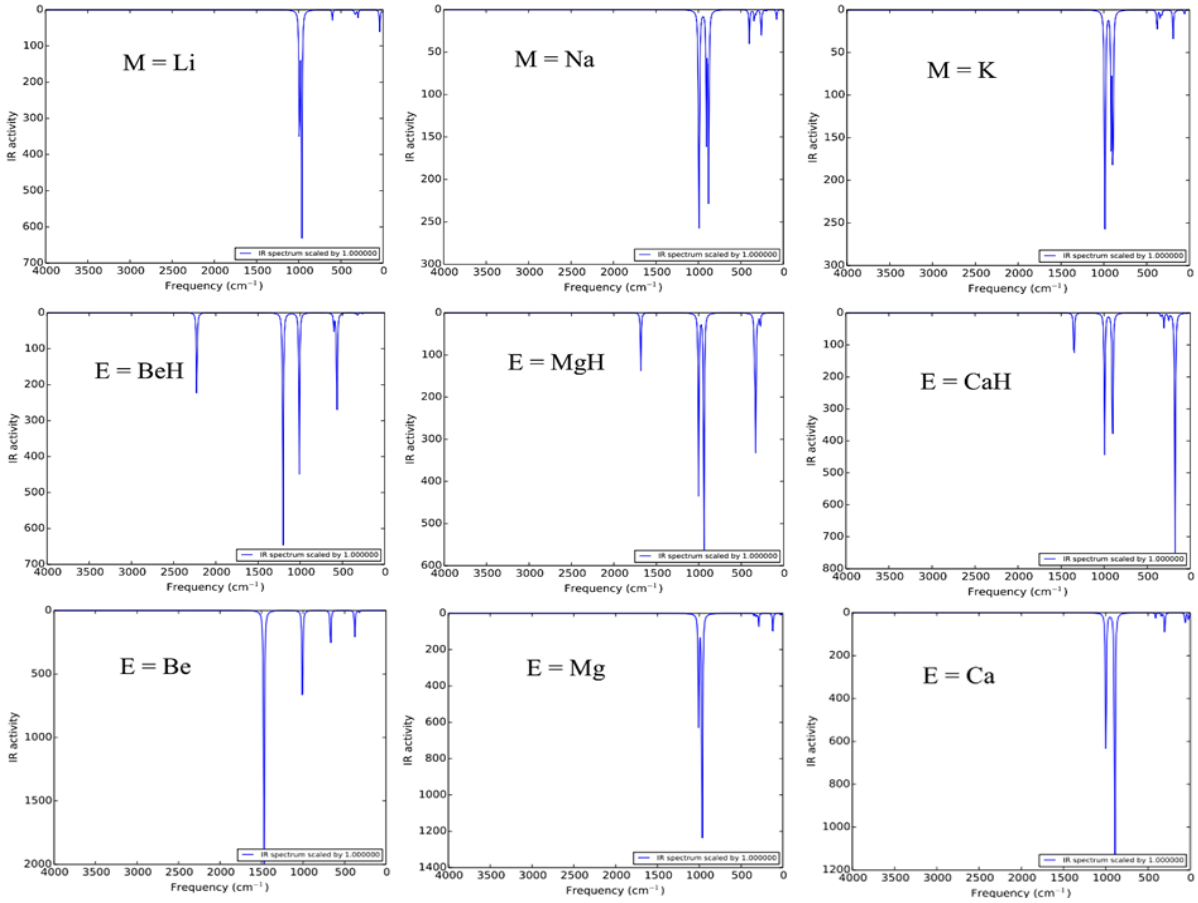

Figure 4. The IR spectra of the molecules under study

E=Mg: 22.9844, 27.4837, 42.5574, 45.8832, 119.4251, 120.0048, 140.9667, 280.1795, 280.6115, 288.5138, 288.9073, 317.2705, 343.8240, 344.1129, 344.4504, 344.7491, 350.3509, 544.6465, 940.7961, 965.0517, 1005.6835, 1006.0097, 1006.4256, 1007.1176, 1007.5823, and 1010.3074.

E=CaH: 37.9318, 41.7578, 176.6030, 176.7000, 251.1466, 305.5716, 306.0089, 340.4308, 341.1189, 358.9602, 901.7175, 989.9184, 994.5915, 995.4690, and 1350.3962.

E=Ca: 5.4792, 19.9817, 21.6657, 40.4487, 42.2583, 59.0397, 59.8319, 124.2208, 299.0772, 300.3881, 302.3492, 303.3488, 303.9943, 340.9414, 341.2529, 341.6756, 341.9989, 344.6829, 409.9966, 892.5962, 914.7980, 993.0544, 993.9059, 997.9111, 998.2273, 998.9302, and 999.2432.

One of the most important techniques in determining the chemical properties of the inorganic molecules is the ultraviolet-visible (UV-Vis) spectrum. Here, the electronic transitions of the studied molecular structures are discussed (Figure 5).

M=Li: UV-Vis [wavelength of electronic transition (nm), energies (cm^{-1}), and electronic transitions]: a) 337.177 nm (29658.018 cm^{-1}), HOMO to LUMO (38%), HOMO to LUMO+1 (27%), HOMO-2 to LUMO (7%), HOMO-2 to LUMO+1 (8%), HOMO-1 to LUMO (8%) and HOMO-1 to

LUOMO+1 (6%). b) 337.122 nm (29662.857 cm^{-1}), HOMO to LUMO (27%), HOMO to LUMO+1 (38%), HOMO-2 to LUMO (8%), HOMO-2 to LUMO+1 (6%), HOMO-1 to LUMO (7%) and HOMO-1 to LUOMO+1 (8%).

M=Na: UV-Vis [wavelength of electronic transition (nm), energies (cm^{-1}), and electronic transitions]: a) 330.261 nm (30279.069 cm^{-1}), HOMO-2 to LUMO+1 (30%) and HOMO to LUOMO (66%).

M=K: UV-Vis [wavelength of electronic transition (nm), energies (cm^{-1}), and electronic transitions]: a. 324.114 nm (30853.340 cm^{-1}), HOMO-2 to LUMO+1 (41%) and HOMO to LUOMO (55%).

E=BeH: UV-Vis [wavelength of electronic transition (nm), energies (cm^{-1}), and electronic transitions]: a) 345.415 nm (28950.665 cm^{-1}), HOMO-3 to LUMO (10%), HOMO-2 to LUMO+1 (10%), HOMO to LUMO+1 (68%), HOMO-3 to LUMO+1 (3%) and HOMO-2 to LUOMO+1 (3%). b) 345.367 nm (28954.697 cm^{-1}), HOMO-3 to LUMO+1 (10%), HOMO-2 to LUMO (10%), HOMO to LUMO (68%), HOMO-3 to LUMO (3%) and HOMO-2 to LUOMO+1 (3%).

E=Be: UV-Vis [wavelength of electronic transition (nm), energies (cm^{-1}), and electronic transitions]: a) 345.695 nm (28927.274 cm^{-1}), HOMO to LUMO+1 (32%), HOMO-1 to LUMO+3 (23%), HOMO-5 to LUMO+3 (4%), HOMO-4 to LUMO+2 (4%), HOMO-3 to LUMO+1 (6%), HOMO-2 to LUMO (6%), HOMO to LUMO+1 (6%) and HOMO to LUOMO+3 (5%). b) 345.675 nm (28928.888 cm^{-1}), HOMO-1 to LUMO (25%), HOMO-1 to LUMO+2 (19%), HOMO to LUMO (13%), HOMO to LUMO+2 (10%), HOMO-5 to LUMO (6%), HOMO-4 to LUMO+1 (6%), HOMO-3 to LUMO+2 (5%) and HOMO-2 to LUOMO+3 (5%).

E=MgH: UV-Vis [wavelength of electronic transition (nm), energies (cm^{-1}), and electronic transitions]: a) 339.876 nm (29422.502 cm^{-1}), HOMO-3 to LUMO+1 (10%), HOMO-2 to LUMO (10%), HOMO to LUMO (60%), HOMO-3 to LUMO (4%), HOMO-2 to LUMO+1 (3%) and HOMO to LUOMO+1 (7%). B) 339.867 nm (29423.301 cm^{-1}), HOMO-3 to LUMO (10%), HOMO-2 to LUMO+1 (10%), HOMO to LUMO+1 (60%), HOMO-3 to LUMO+1 (3%), HOMO-2 to LUMO (4%) and HOMO to LUOMO (7%).

E=Mg: UV-Vis [wavelength of electronic transition (nm), energies (cm^{-1}), and electronic transitions]: a) 341.571 nm (29276.515 cm^{-1}), HOMO-1 to LUMO (22%), HOMO-1 to LUMO+2 (20%), HOMO to LUMO (12%), HOMO to LUMO+2 (11%), HOMO-5 to LUMO (4%) and HOMO-4 to LUOMO+1 (4%).

E=CaH: UV-Vis [wavelength of electronic transition (nm), energies (cm^{-1}), and electronic transitions]: a) 365.873 nm (27331.899 cm^{-1}), HOMO to LUMO (100%). b) 365.582 nm (27353.676 cm^{-1}), HOMO to LUMO+1 (100%). c) 338.096 nm (29577.362 cm^{-1}), HOMO-3 to LUMO+1 (11%),

HOMO-2 to LUMO (11%), HOMO-1 to LUMO (63%), HOMO-3 to LUMO (3%), HOMO-2 to LUMO+1 (3%) and HOMO-1 to LUOMO+1 (4%).

E=Ca: UV-Vis [wavelength of electronic transition (nm), energies (cm^{-1}), and electronic transitions]: a) 339.411 nm (29462.830 cm^{-1}), HOMO to LUMO+1 (23%), HOMO to LUMO+3 (23%), HOMO-5 to LUMO+3 (4%), HOMO-4 to LUMO+2 (4%), HOMO-3 to LUMO+1 (4%), HOMO-2 to LUMO (4%), HOMO-1 to LUMO (6%), HOMO-1 to LUMO+2 (5%), HOMO to LUMO (5%) and HOMO to LUOMO+2 (5%). b) 339.383 nm (29465.250 cm^{-1}), HOMO-1 to LUMO+1 (31%), HOMO-1 to LUMO+3 (29%), HOMO-5 to LUMO+1 (3%), HOMO-5 to LUMO+3 (2%), HOMO-4 to LUMO (3%), HOMO-4 to LUMO+2 (2%), HOMO-3 to LUMO+3 (2%), HOMO-2 to LUMO (2%) and HOMO-1 to LUOMO (2%).

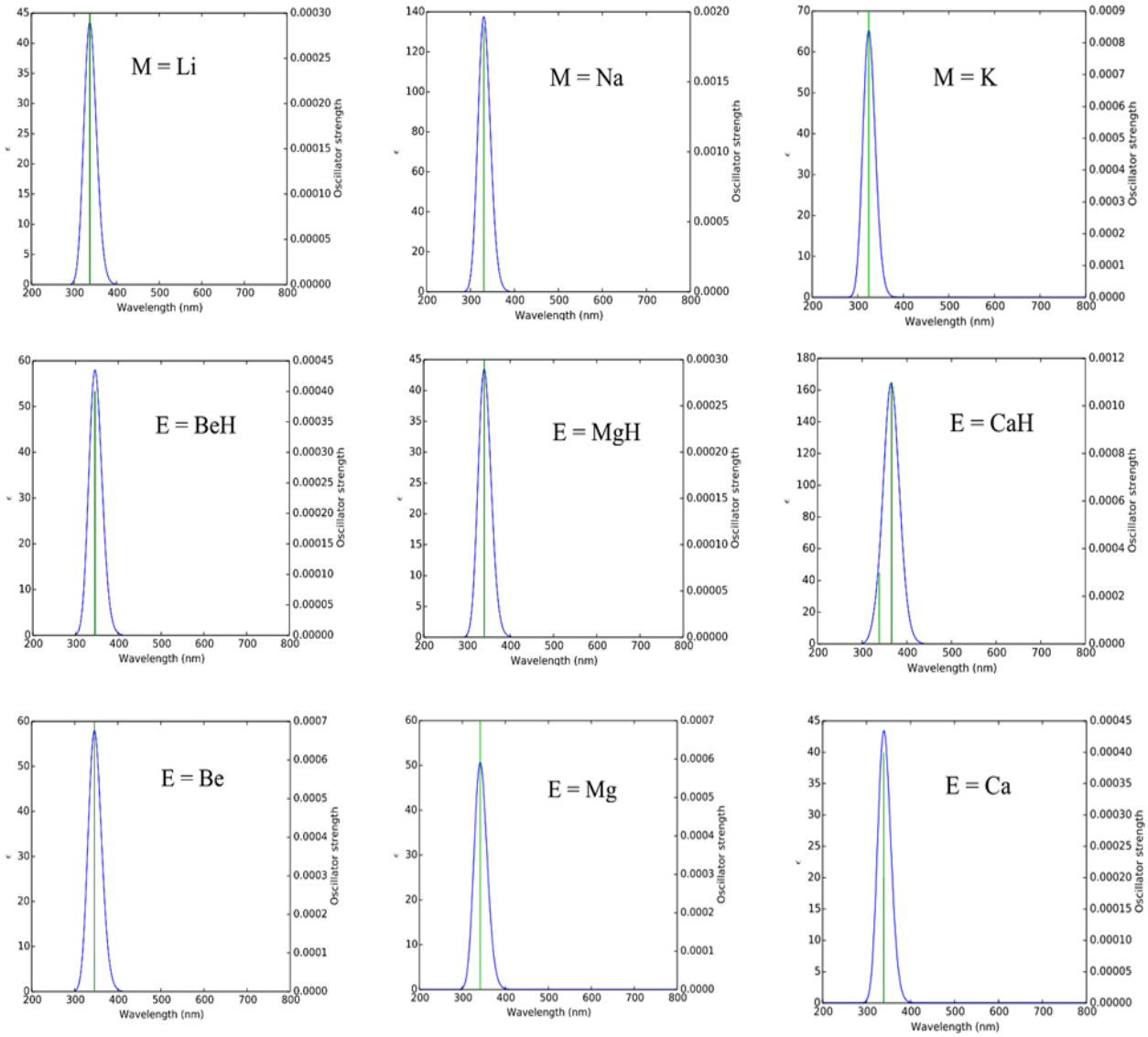

Figure 5. The UV-Vis spectra of the molecules under study

Conclusions

The main aim of the present article is to study the structural and electronic properties and spectroscopy analyses (IR and UV-Vis) of the alkali (Li, Na and K) and alkaline earth (Be, Mg and Ca) salts of the pertechnetate oxoanion ($^{99m}TcO_4^-$) as the convenient water-soluble sources of the radioactive element technetium using density functional theory (DFT) method by B3LYP functional with 6-31+G(d,p) basis set. It is necessary to say that the Lanl2DZ effective core potential basis set for the technetium-99m radioisotopes. The geometry optimization of the title compounds indicates that the strength order of M-O (M=Li, Na and K) bonds is Li–O>Na–O>K–O. On the other hand, E–O3 (E=Be, Mg and Ca) bond lengths increasing and Tc–O3 bond lengths decreasing of the monoanion and dianion salts of alkaline earth metals are observed. In the FMO investigation, the electrophilicity index orders of the molecules under study Na>Li>K and Be (BeH)>Mg (MgH)>Ca (CaH) show that the sodium and beryllium salts of pertechnetate anion are more susceptible to react with electron-donating compounds. Also, the molecular electrostatic potential (MEP) graphs show that the oxygen atoms, technetium-99m radioisotopes and the cations have negative, zero and positive electrostatic potentials, respectively.

Acknowledgments

The corresponding author is grateful to Mr. Hossein Abbasi for providing valuable suggestions.

References

[1]. Elizarov A.M., Dam R.M., Shin Y.S., Kolb H.C., Padgett H.C., Stout D., Shu J., Huang J., Daridon A., Heath J.R. *J. Nucl. Med.,* 2010, **51:**282

[2]. Nabati M. *Chem. Method.,* 2018, **2:**223

[3]. Bhattacharyya S., Dixit M. *Dalton Trans.,* 2011, **40:**6112

[4]. Nabati M. *J. Phys. Theor. Chem. IAU Iran.,* 2017, **14:**49

[5]. Boyd R.E. *Radiochimica Acta.,* 1982, **30:**123

[6]. Bayne V.J., Forster A.M., Tyrrell D.A. *Nucl. Med. Commun.,* 1989, **10:**29

[7]. Green C.H. *J. Med. Phys.,* 2012, **37:**66

[8]. Briner W.H., Harris C.C. *J. Nucl. Med.,* 1974, **15:**466

[9]. Nabati M. *Chem. Method.,* 2017, **1:**121

[10]. Nabati M., Mahkam M. *Inorg. Chem. Res.,* 2016, **1:**131

[11]. Cho A.E., Guallar V., Berne B.J., Friesner R. *J. Comput. Chem.,* 2005, **26:**915

[12]. Beierlein F., Lanig H., Schurer G., Horn A.H.C., Clark T. *Mol. Phys.,* 2003, **101:**2469

[13]. Nabati M., Mahkam M. *Org. Chem. Res.,* 2016, **2:**70

[14]. Nabati M., Mahkam M. *Silicon,* 2016, **8:**461

[15]. Saidi W., Abram T., Bejjit L., Bouachrine M. *Chem. Method.,* 2018, **2:**247

[16]. Sadegh H., Sayadian M. *Chem. Method.,* 2018, **2:**239

How to cite this manuscript: Mehdi Nabati.Insight into the structural and spectral (IR and UV-Vis) properties of the salts of alkali (Li, Na and K) and alkaline earth (Be, Mg and Ca) metals with pertechnetate oxoanion ($^{99m}TcO_4^-$) as the convenient water-soluble sources of the radioactive element technetium.*Asian Journal of Green Chemistry*, 3(2) 2019, 258-270. DOI: 10.22034/ajgc.2018.144525.1096